The Colossal Piezoresistive Effect in Nickel Nanostrand Polymer Composites and a Quantum Tunneling Model

Oliver K. Johnson[1]**, Calvin J. Gardner**[1]**, David T. Fullwood**[1]
Brent L. Adams[1]**, Nathan Hansen**[2] **and George Hansen**[2]

Abstract: A novel nickel nanostrand-silicone composite material at an optimized 15 vol% filler concentration demonstrates a dramatic piezoresistive effect with a negative gauge factor (ratio of percent change in resistivity to strain). The composite volume resistivity decreases in excess of three orders of magnitude at a 60% strain. The piezoresistivity does decrease slightly as a function of cycles, but not significantly as a function of time. The material's resistivity is also temperature dependent, once again with a negative dependence.

The evidence indicates that nickel strands are physically separated by matrix material even at high volume fractions, and points to a charge transport mechanism that causes a large change in conductivity for a small relative change in the distance between filler particles. Combined with the temperature dependence data, this suggests that conduction in this composite material may be dominated by quantum tunneling effects. Based upon a statistical model of junction character distribution, a quantum tunneling percolation model is applied that accurately reflects the mechanical and thermal trends.

Keywords: Nickel Nanostrands, Piezoresistive, Tunneling, Percolation, Probable Orientation Analysis, Junction Character Distribution Function, CMC.

1   Introduction

At the forefront of many technological advances are new or enhanced materials. Multifunctional materials, in particular, are providing benefits in the form of property combinations supplied by the various constituents, or novel properties arising from the formulation. One particularly fruitful area of development has been the tailoring of electrical properties of composites via the addition of nano-particulates. Carbon nanotubes, carbon black, nano-silver and nano-nickel are among the many

[1] Brigham Young University, Provo, UT, U.S.A.
[2] Conductive Composites Company, LLC., Midway, UT, U.S.A.

materials used to increase electrical conductivity for applications such as structural health monitoring, lightning strike protection, electrostatic discharge protection and electromagnetic shielding.

Not surprisingly, many of these conductive composites also exhibit a piezoresistive effect, which potentially provides yet another extremely useful function. Application of extreme strain or of severe cycling in structures might be identified and rectified before structural damage occurs. Furthermore, the strain range of polymeric matrix materials is often significantly greater than the limits of traditional piezoresistive materials such as metals or semiconductors; thus the potential applications increase dramatically. However, the piezoresistive properties of conductive composites have tended to be variable and unstable; thus they are not conducive to sensor applications that rely upon repeatability and the ability to calibrate the material response.

Nickel nanostrand polymer composites are particularly interesting multifunctional materials, producing highly conductive composites at low filler volume fractions, providing both unique electric and magnetic properties, and exhibiting a negative gauge factor as a piezoresistive material. Unlike many other piezoresistive materials, the resistance of these composites *decreases* remarkably with strain [Hansen (2007), Johnson, Gardner, Fullwood, Adams and Hansen (2009)]. This paper reports on both the remarkable piezoresistive properties exhibited by nano-nickel composites, and on a tunneling-percolation model that focuses on the junction character of the composite structure and captures the piezoresistive behavior (including related temperature effects).

2   Conductive Nanocomposites (CNCs)

Electrical properties of conductive nanocomposites (CNCs) have predominantly been modeled using percolation theory, rather than alternatives such as the effective medium theory, due to the high contrast in electrical properties between the matrix and the filler [Grunlan, Gerberich and Francis (2001), Gul (1996), Jing, Zhao and Lan (2000), Kyrylyuk (2008), Wang and Ogale (1993)]. Percolation theory models the connectivity across an infinite sample of a network structure. In the case of CNCs, the network is provided by the conductive particulates. The underlying theory suggests that as the volume fraction of conductive material increases, locally connected clusters of the conductive material will grow until a fully connected path exists across the whole sample at the percolation threshold. In the region above this threshold the available conductive paths across the sample increase, and the resistivity obeys a power law given by [Grimmett (1999)]:

$$\sigma \sim (p - p_c)^{\tau} \tag{1}$$

where p represents the volume fraction of conductive material, p_c represents the percolation threshold, and τ is a universal constant, which for 3-D networks approximately equals 2.

Basic percolation theory assumes that two components of a network are either connected or not connected; it does not account for two conductors, or clusters, being 'almost' connected. Yet, in a CNC, it is well known that the resistivity is dominated by resistance at the small gaps between neighboring conductors. We will refer to these contact points as junctions. For junctions with very small gaps (on the order of 1 nm) the junction resistance must consider a possible quantum tunneling effect [Simmons (1963)]. A combined tunneling-percolation model has been applied to carbon nanocomposites with reasonable results [Balberg (1987), Rubin, Sunshine, Heaney, Bloom and Balberg (1999)].

The tunneling model is particularly attractive when applied to the study of the piezoresistive effect in CNCs [Radhakrishnan (1994), Rakowski and Kot (2005), Taya, Kim and Ono (1998)]. The exponential change in resistance at a junction with increasing gap provides a logical explanation for large resistivity variations with strain. Two recent studies illustrate the approach, and potential issues that might arise. The first considers carbon nanotubes in epoxy, at relatively low strains ($\sim$1%), and concludes that the tunneling effect dominates the piezoresistive behavior [Hu, Karube, Yan, Masuda and Fukunaga (2008)]. However, the change in resistivity with strain is opposite to that seen in the nano-nickel composites reported below, and hence the model is incorrect for this case. The second study considers piezoresistivity of a carbon black loaded elastomer under hydrostatic pressure, and concludes that the piezoresistive effect is dominated by the change in effective volume fraction under the applied strain rather than the tunneling effect [Zhou, Song, Zheng, Wu and Zhang (2008)]. Furthermore, the experimental results are generally unstable, and require adjustment as residual strain accumulates in the material. In either case, the piezoresistive effect is nowhere near as dramatic as that seen in the nickel, and clearly significant modifications to the model are required.

We note two significant areas of uncertainty in quantum tunneling calculations that will not be resolved in this paper, but which we hope to address in more detail in the future. The first involves the barrier height to electron flow at the junctions in the tunneling model. Previous measurements have been reported for various materials using atomic force microscopes [Chen and Hamers (1991), Louis and Sethna (1995)], but this is a difficult measurement that is not routinely performed. The second is the thickness of the adsorbed (immobilized) layer of matrix material on the conductive network which is expected to greatly affect the junction gap distribution. Litvinov estimates this layer to be approximately one to two diameters of the monomer chain [Litvinov and Steeman (1999)], leading to a layer on the

order of 1 nm for many polymers.

3   Nano-Nickel Composites

The nickel nano material reported in this paper is produced using a proprietary chemical vapor deposition (CVD) process that results in a tree-like structure of nanostrands with a volume fraction of less than 0.5% nickel [Hansen (2007)], as shown in Fig. 1. The initial volume fraction of the original CVD product, compared to that of the resulting nickel structures, is clearly critical in creating the high level of connectivity seen in the resulting nanocomposites. The fully connected mass of CVD nickel is broken into smaller components that retain an interconnected branching structure; fully connected clusters are sometimes termed 'animals' (from terminology in percolation theory) [Balberg, Wagner, Goldstein and Weisz (1990)]. When incorporated into polymer systems, the branching structure results in composites with unusual properties. Of particular interest, the electrical conductivity is higher than would be expected for the volume percent of nickel nanostrands, and the conductivity changes dramatically under mechanical load. We note that it is well known that the geometry of the conducting material has a strong effect on the response of the resulting composite [Dalmas, Dendievel, Chazeau, Cavaille and Gauthier (2006), Gao and Ma (2008), Jing, Zhao and Lan (2000), Rubin, Sunshine, Heaney, Bloom and Balberg (1999)].
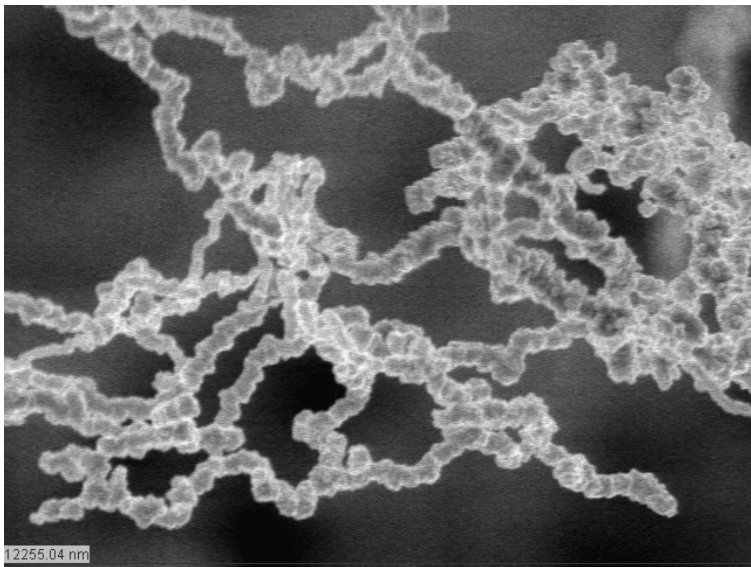

Figure 1: A typical interconnected nickel nanostrand structure.

Previous efforts towards modeling conductivity of nickel nanostrand (NiNs) composites have used techniques including both effective medium and percolation theories [Li, Gao and Fielding (2007)]. However, to the authors' knowledge, these models have not been extended to consider piezoresistive behavior of NiNs composites. As mentioned above, perhaps the most promising model for piezoresistive behavior involves tunneling-percolation models [Balberg (1987), Hu, Karube, Yan, Masuda and Fukunaga (2008), Rubin, Sunshine, Heaney, Bloom and Balberg (1999), Zhou, Song, Zheng, Wu and Zhang (2008)]. Most existing models predict an increase in resistivity as the composite is strained in tension [Wymyslowski, Santo-Zarnick, Friedel and Belavic (2004)], based on the assumption that the distance between filler particles increases; and similarly they predict a decrease in resistivity in compression due to a decrease in distance between filler particles [Bloor, Graham, Williams, Laughlin and Lussey (2006), Zhou, Song, Zheng, Wu and Zhang (2008)]. NiNs composites, however, demonstrate a decrease in resistivity with strain both in tension and compression [Hansen (2007)]. It is apparent that the mechanism for piezoresistivity in these composites is not well understood.

In this paper we build upon the tunneling-percolation model, paying close attention to the strain field in the neighborhood of junctions. A junction character distribution function is assumed that incorporates both the gap between the conductors and the orientation of the unit vector connecting the closest point between them. For the nano-nickel structure it is assumed that the unit vectors lie randomly on the unit sphere; clearly this would not be the case for many carbon nanotube composites if alignment of the tubes occurs during processing. The strain field in the region of such junctions is analyzed using finite element modeling, and an accompanying statistical approach. The resultant assessment of the resistance change on the junction distribution is fed into the tunneling-percolation model, resulting in a good prediction of the resistivity change apparent in the nano-nickel composite under strain – correctly predicting the negative gauge factor. The temperature characteristics of the material are also well modeled in terms of effects on tunneling resistance.

We first present the results from actual material testing, including the effects of cycling and time on the nano-nickel composite. The electrical properties of the nickel nanocomposite were characterized, for a range of volume fractions and polymeric matrix materials, under various mechanical loads and temperatures. The structure of the nickel animals and junctions was examined both in and out of the polymer matrix using microscopy and statistical techniques. And finally, an analysis and design framework was developed based upon the mathematical models mentioned above for analysis of structure-property relations, and improvement in performance of nanocomposites.

4   Materials and Methods

Nano-nickel composites have been known to have highly desirable electrical properties since their relatively recent introduction. Fig. 2 shows resistance properties for several nanocomposites, emphasizing the dramatic improvements in conductivity when NiNs are included. Various matrix and filler materials have been used in conductive and piezoresistive composites in the past, with a significant effect on the resultant properties [Balberg (2002), Bigg (1977), Kirkpatrick (1973), McLachlan, Chiteme, Park, Wise, Lowther, Lillehei, Siochi and Harrison (2005), Simmons (1963), Tang, Chen, Tang and Luo (1996), Wescott, Kung and Maiti (2007)].
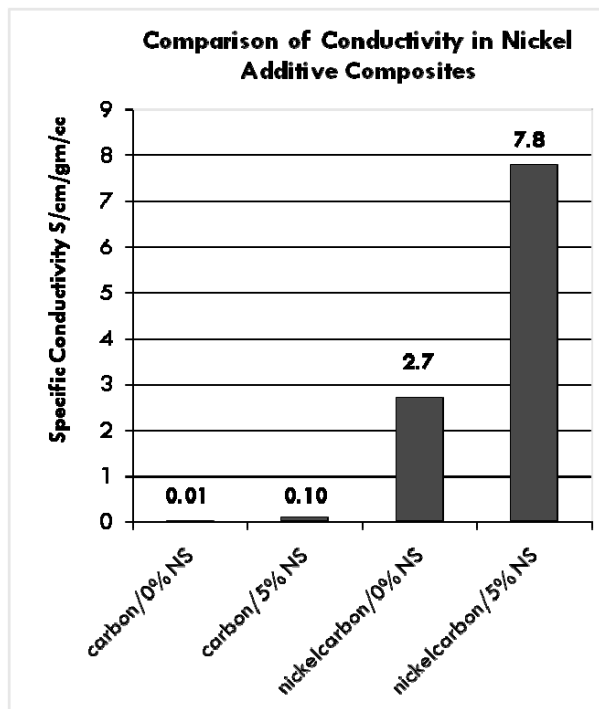

Figure 2: Specific conductivity for 3501-6 epoxy resin with carbon fibers (carbon) or 20 wt% nickel on carbon fiber (nickelcarbon) with and without nickel nanostrands (NS). Data courtesy of Conductive Composites Company, LLC.

The piezoresistive nano-nickel composites used in this study were developed by first comparing silicone and polyurethane matrix materials. Next, the volume percent of nickel nanostrands was varied from 5 percent to 17.5 percent. Finally, additives were tested for improved properties including nickel coated carbon nan-

otubes, nickel coated carbon flakes, and carbon black. At each stage copper mesh contacts were infused in the samples for improved and consistent connectivity.

The samples were pulled in tension, and resistance measurements were taken at a step size of 12 mm. The polyurethane matrix sample was pulled to 29% strain and the silicone-based sample to 63%. The optimized composition of silicone and nanostrands was then cycled in tension to determine whether or not the piezore-sistivity would change as a function of cycle number (as generally occurs with previously reported materials [Zhou, Song, Zheng, Wu and Zhang (2008)]). Cycling was then applied daily over a period of 28 days to determine whether the piezoresistive effect would change over time.

It has been observed that the conductivity of composites with conductive additives and polymer matrices varies with temperature [Bigg (1979), Mehbod (1987)]. Therefore the piezoresistivity of the composite was also measured as a function of temperature between 260 Kelvin and 325 Kelvin.

5   Results

The resistivity of a sample is given by:

$$\rho = R\frac{A}{L} \tag{2}$$

where R is the measured resistance, L is the sample length, and A is the cross sectional area. Typical resistivity measurements for strained polyurethane and silicone matrix samples are shown in Figs. 3a and 3b.

The resistivity of the composite consisting of 12.5 volume percent nickel nanostrands in a polyurethane matrix was initially relatively low, and decreased nearly linearly as a function of strain before reaching a minimum just prior to failure at 28.7% strain. These results are presented in Fig. 3a.

Unlike the polyurethane composite sample, the silicone matrix sample containing 15 volume percent nickel nanostrands had an initially high resistivity. However, the piezoresistive effect in the silicone sample was much more pronounced. At just over 60% elongation, the resistivity had decreased in excess of three orders of magnitude at mechanical failure. The results are presented in Fig. 3b.

Silicone offers a number of advantages as a matrix material. Sylgard 184 silicone (used in this study) has a tensile strength of 1.8 MPa and is capable of a 160% elongation prior to failure [Choi and Rogers (2003)]. This elongation is decreased significantly by the addition of the nano-nickel; nevertheless, the random branching structure of nickel nanostrands allows the composite material to remain highly compliant. Hence, the resultant composite displays a high strain range that is likely
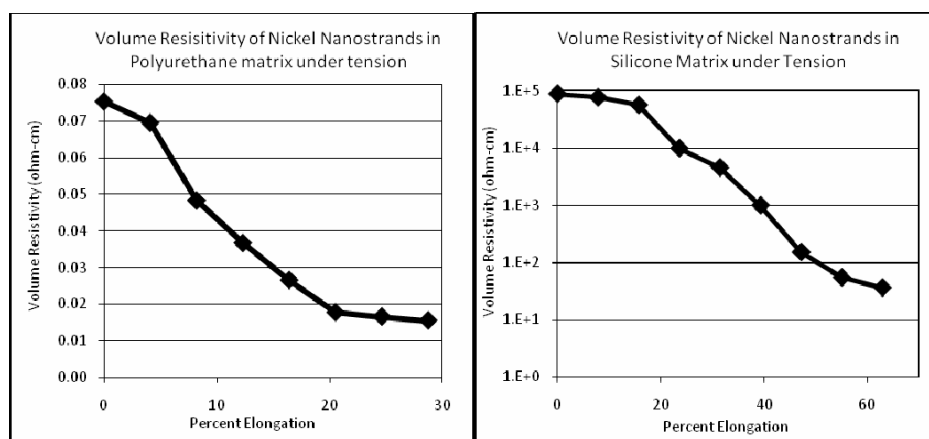
Figure 3: a) A quasi-linear decrease in resistivity for NiNs-PU composite; b) Colossal piezoresistive effect in NiNs-silicone composite.

to be of significant advantage in some multifunctional applications. By way of contrast, when nickel coated carbon nanotubes are used as a conductive additive the composite's elongation is drastically reduced.

Figure 4 shows a comparative graph of the gauge factor ($\Delta R/R = G\varepsilon$, where R is the resistance and G is the gauge factor) of composites including two different polymers, two different conductive additives, and various volume percent concentrations. The results shown in Fig. 4 illustrate that the higher the concentration of nickel nanostrands in a material, the more pronounced the piezoresistive effect.

The silicone matrix composite containing 15 volume percent nickel nanostrands exhibits a piezoresistive effect over two orders of magnitude higher than the next closest sample. It should be noted that in excess of 15 vol% filler, the composite's mechanical properties degrade sharply [Nurazreena, Hussain, Ismail and Mariatti (2006), Schadler, Giannaris and Ajayan (1998)]. Thus, the optimal filler composition used in the work reported later in this paper was 15 volume percent nickel nanostrands in a silicone matrix material. Tested samples exhibited an impressive 2400% increase in conductivity at 60% elongation. We note also that the addition of 15 vol% nickel nanostrands resulted in an increase in elastic modulus from 1.8 MPa [Choi and Rogers (2003)] for neat Sylgard 184 to ~6.5 MPa for the composite material.

The nickel nanostrand-silicone composite exhibits a slowly increasing resistivity as a function of cycle number. When pulled at 1 Hz from 0 to 20% elongation through 150 cycles, the resistivity increased from approximately 2700 ohm-cm to nearly
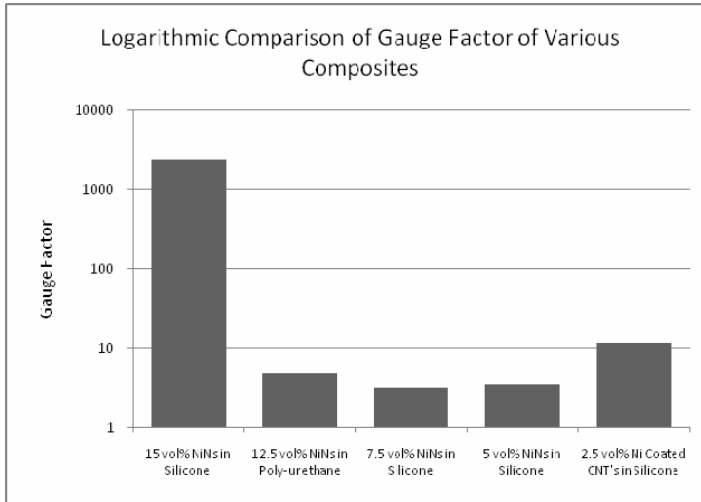
Figure 4: The colossal piezoresistivity of the NiNs-silicone sample is orders of magnitude greater than other samples tested. CNT = Carbon Nanotubes.

3300 ohm-cm as shown in Fig. 5. The sudden increase near the end of the graph is due to the macroscopic mechanical failure of the sample.

Additionally, the composite did not show any significant change in piezoresistivity as a function of time. The composite was strained to 20% elongation once daily for 28 days. The volume resistivity was found to have a very slight downward trend that may be easily attributed to random discrepancies in the measurements rather than any indication of time-dependence. These effects are not discussed in detail below, and would require some complex micromechanics to explain. It is likely that micromechanical damage occurs during the cycling in Fig. 5, finally resulting in the failure of the sample. During the daily cycles it is possible that creep compensates for the potential local damage, resulting in little change in the resistivity for this test. We note that typical room temperature stress relaxation experiments have been reported to have a 22% decrease in macroscopic stress for a 24 hour period [Stein (1988)].

Previously, composites consisting of conductive fillers in a nonconductive matrix have exhibited an increase in resistivity with increasing temperature and a declining resistivity with decreasing temperature [Guo (2007)]. Additionally, metals typically are governed by the Bloch–Grüneisen formula which predicts an increasing resistivity with increased temperature [Deutsch (1987)]. The nickel nanostrand composite is also affected by temperature but, interestingly, the result is precisely
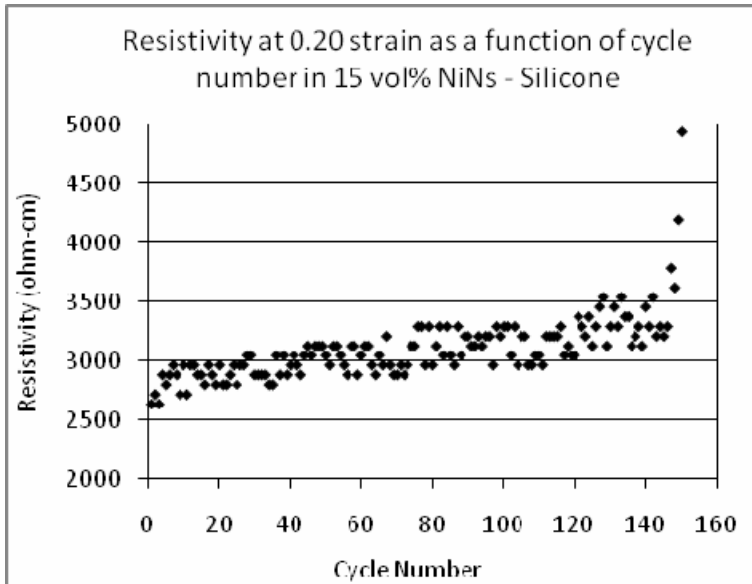
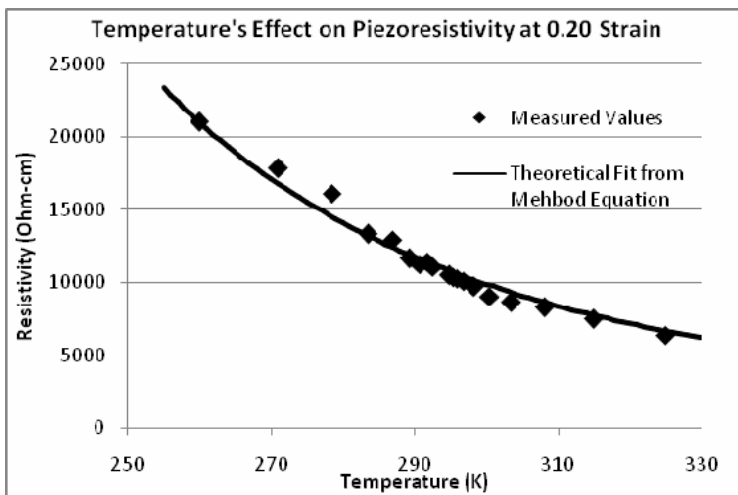Figure 5: Resistivity change for 15 vol% NiNs composite cycled at 1 Hz.

Figure 6: Resistivity vs. temperature for 15 vol% nickel nanostrands in silicone.

opposite. At 20% elongation the optimized polymer-silicone composite exhibits a decreasing resistivity with increasing temperature as shown in Fig. 6.

The experimental values follow the equation for temperature dependence in conductive polymer composites proposed by Mehbod [Mehbod (1987)]:

$$\ln \rho \sim T^{-\alpha} \tag{3}$$

where ρ is the volume resistivity in ohm-cm, T is temperature in Kelvin, and α is a fitting parameter chosen to be 0.55 for the results in Fig.6. As shown in Fig. 6, equation (3) gives the correct form and a close approximation to the measured values for resistivity at various temperatures. Mehbod's model assumed 'electron hopping', and strongly supports the quantum tunneling model to be introduced below.

In summary, a colossal piezoresistive effect was observed in an optimized composite containing 15 volume percent nickel nanostrands in a silicone matrix. The gauge factor is negative, in contrast to positive gauge factors reported in previous piezoresistive nanocomposites. The effect exhibits only slight degradation as a function of cycles, and insignificant change with time. Additionally, the conductivity of the material is dependent on temperature, and experiences an increasing conductivity as temperature is increased; this effect is opposite of that observed in many other materials. The next section analyzes these measured phenomena.

6 Modeling

6.1 Nickel Nanostrand Structural Analysis

In order to arrive at structural parameters for a detailed model, characterization of unprocessed nickel nanostrand structures was performed. Fifty distinct SEM images of nickel nanostrands were analyzed. The images were chosen for their clarity and distinctive structures. The results define nickel nanostrand size, shape, and structure more completely than has previously been reported.

Three important values were extracted from the data. First, the distribution of aspect ratios (length/diameter) of branched members is represented in Fig. 7a. Second, the branching ratio (distance between branches / stem diameter) is represented in a similar manner in Fig. 7b. Finally, the diametric change ratio distribution (branch diameter/stem diameter) is represented in Fig. 7c. This latter distribution very closely follows a normal distribution. Branching angle is still being studied, though preliminary results indicate an entirely random branching angle distribution with no angular preference.

The thickest branch recorded was approximately 3000 nm in diameter and the thinnest observed branch was approximately 100 nm thick. These two values are
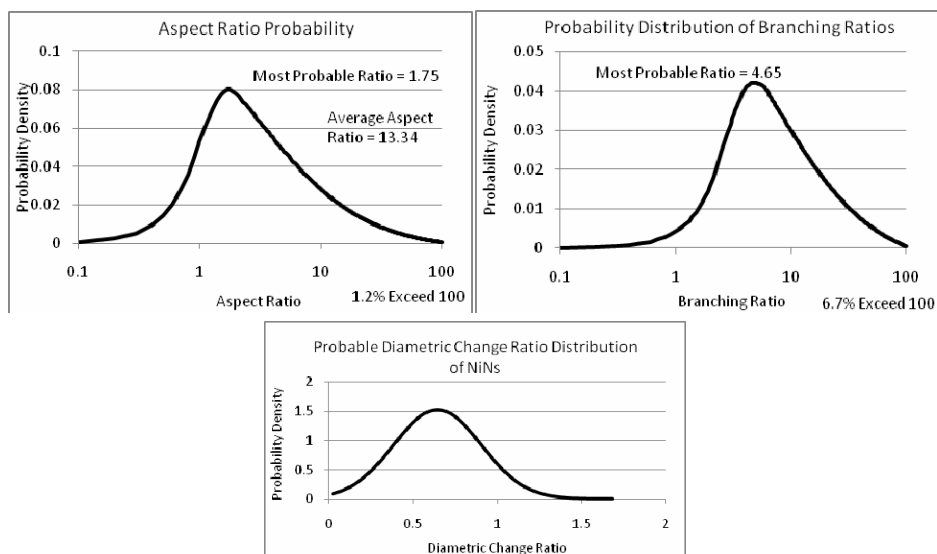
Figure 7: a) Statistics of observed aspect ratios; b) Statistics of observed branching ratios; c) Statistics of observed diametric change ratios.

used as limiting factors for a full nickel nanostrand reconstruction. With the base strand set at 3000 nm, the three shape determining ratios can be applied to reconstruct and study the nanostrand structure.

6.2 Junction Character Parameters

The dramatic reduction in resistivity with strain reported above suggests two things. Firstly, the dominant mechanism in the resistance between conductors is highly sensitive to changes in the gap; and secondly, the original gaps must be small to result in a significant relative change under strain. Nano-nickel composites have been produced with a variety of matrix materials. The percolation threshold is generally low (less than 1 vol% nickel), and good conductivity is generally achieved by 10 vol%. The fact that the silicone material still has poor conductivity at 15 vol% suggests a polymer barrier between nickel branches that prevents good conduction across junctions. Previous work has identified an adsorbed, or immobilized, layer of polymer in nanocomposites that acts as an insulator at potential junctions. The thickness of these layers tends to be approximately 1-2 diameters of the monomer chain, and are generally of the order of 1 nm thick [Litvinov and Steeman (1999)]. Quantum tunneling starts to become significant when junction gaps are reduced

to around 1 nm [Erkoc (2006)]. Thus, our hypothesis is that at 15 vol% nano-nickel, there are adequate available junctions for significant conductivity, but that the junctions generally have gaps greater than 1 nm. As the material is strained, a significant number of the gaps shorten to within the critical range of less than 1 nm.

The junction character is defined by a series of parameters that will have different levels of impact on the junction conductivity. If we assume perfect bonding between the matrix and nano-nickel, then the most important parameter is the gap length, d, across the junction. The conductivity is also affected by the area of conductor available on either side of the gap, which is related to the radius of the strands, and to the relative angles (or misorientation, given by inclination and azimuthal angles α, β) that the strands make with each other (for example, if the strands were aligned in a parallel fashion, this would clearly lead to higher conduction than if they were aligned orthogonally with respect to one another). Finally, the angle that the junction vector (defined as the unit vector connecting the two closest points of the conductors, and given by θ, φ) makes relative to the applied strain is the determining factor in the evolution of junction parameters under strain.

In order to develop a more concrete picture of the nano-nickel structure, fifty NiNs structures were statistically assembled from the three descriptive ratios derived above. While the structures exhibited a wide size range, the average animal contained on the order of 10^{-16} m^3 of nickel. This means that at 15 vol% of nickel there are approximately 10^{14} nickel nanostrand structures per cubic meter of composite. However, due to the complexity of modeling the position and orientation of NiNs structures in the matrix with respect to one another, it is difficult to determine whether or not there are enough potential junctions for quantum tunneling to be a significant factor in the piezoresistivity. In order to confirm the potential existence of these junctions, a 10 cubic micron section of the optimized composite was imaged on a FIB-SEM (Focused Ion Beam Scanning Electron Microscope) using 100 slices each 100 nm apart. The resulting images exhibit a large number of potential tunneling junctions. Fig. 8 shows a number of these potential tunneling junctions, where a thin layer of silicone exists between the lighter nickel regions. Based on our numerical simulations and empirical investigations it is reasonable to conclude that quantum tunneling can have a profound impact on the conductivity of the composite.

6.3   Effect of Strain on Junction Character

We now consider the effect of strain on the junctions described above. The gaps of junctions with junction vectors aligned to an applied tensile strain will lengthen, while those with vectors orthogonal to the tensile axis will shorten. Hence the 'texture' of the junction vectors (i.e. the distribution of junction vector angles θ and
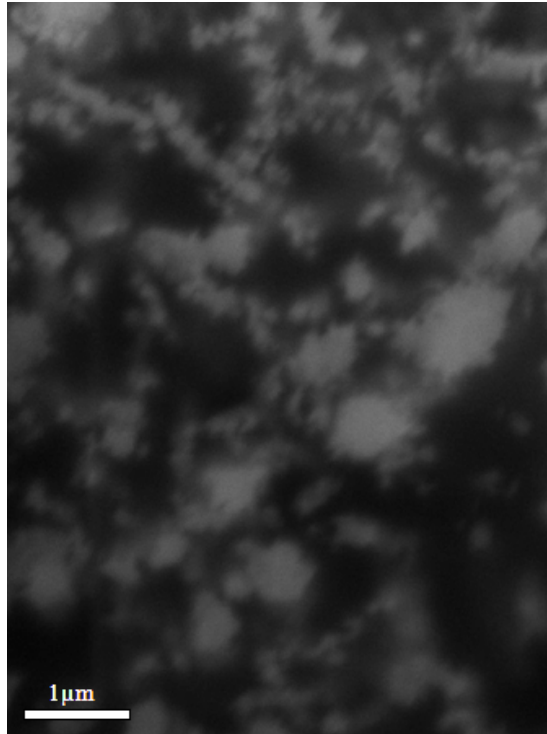
Figure 8: Potential quantum tunneling junctions revealed by FIB-SEM. Dark areas are silicone, lighter areas are nickel nanostrands.

φ) is critical to the determination of the statistical junction character evolution with strain. This idea is completely general, but the texture will be greatly influenced by the original shape of the nano filler and the manufacturing techniques used to create the composite. The process used to create the NiNs-silicone composite is likely to produce a fairly random texture (i.e. the distribution of junction vectors is approximately constant on the unit sphere).

Figure 9 illustrates the response of a unit sphere subjected to a tensile strain, ε_L, along the z-axis. If the material is assumed to be isotropic, the radius at a given angle, ϕ, from the z-axis, after applying the deformation is given approximately by:

$$r(\varphi) = \frac{(1+\varepsilon_L)(1+\varepsilon_L \nu)}{\sqrt{(1+\varepsilon_L)^2 \sin^2 \varphi + (1+\varepsilon_L \nu)^2 \cos^2 \varphi}} \tag{4}$$

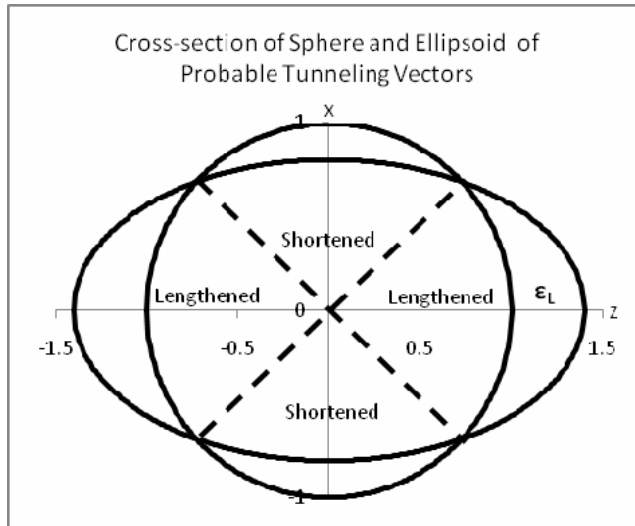where ν is the Poisson's ratio. For a random distribution of unit vectors, 71%

Figure 9: Cross-section of the effect of strain on the distribution of tunneling vectors.

will be shortened (all those within the triangular torus about the z-axis) under the applied strain.

The initial distribution of vector lengths on the unit sphere is simply the delta function at $r = 1$. Figure 10 shows the probability distribution of junction vector lengths after deformation for various levels of strain. The related change in gap for a particular junction is amplified due to the high stiffness of the nickel relative to the silicone matrix, and is dependent upon the entire set of junction parameters introduced earlier. Finite element calculations were performed, for the parallel case, to determine the critical gap length that would shorten to within the critical distance for tunneling (Fig.11). These results show that strands of nickel separated by a thin layer of silicone, up to 15 nm thick, can close to less than 1 nm under 60% tensile strain; such junctions thus become highly conductive.

6.4 Resistivity as a Function of Quantum Tunneling

Nanoscopic junctions between the branches of individual nickel nanostrands can be considered, for charge transport purposes, as similar electrodes separated by a thin insulating film. Each junction is treated as an electrical potential barrier with height λ (eV) – given by the difference in Fermi energies between the silicone and nickel – and width d (Fig. 12a).

As an incident electron impacts the boundary between the nickel and the silicone its
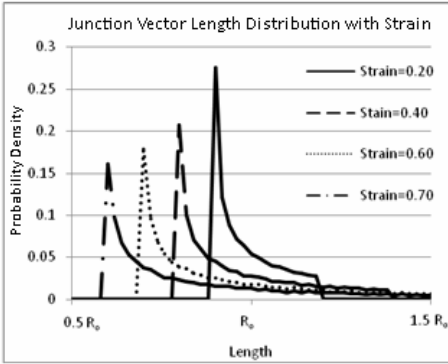
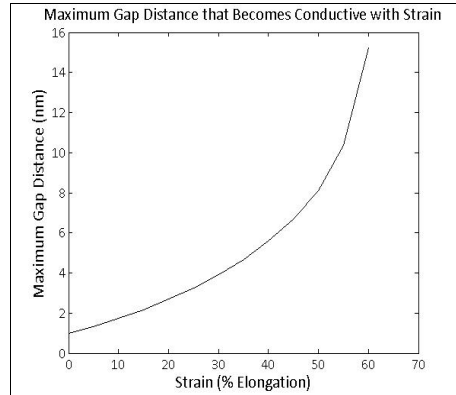Figure 10: Distribution of junction vector lengths with strain. Ro is the unstrained unit sphere radius.

Figure 11: Maximum length junction vector that will become conductive at a given strain.
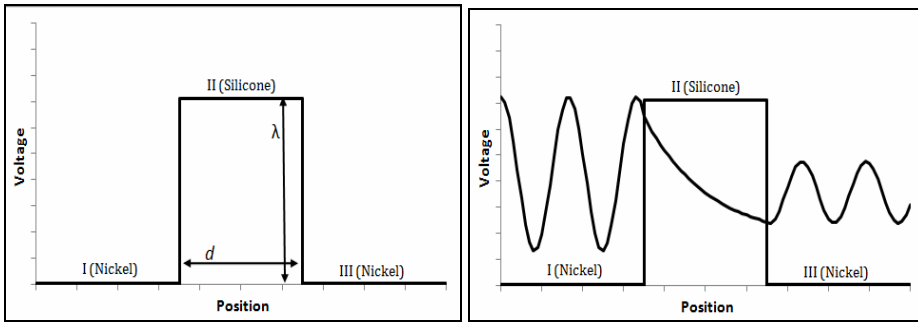

Figure 12: a) Silicone provides a barrier of height lambda between two nickel strands; b) The probability of transmission decreases with barrier width.

behavior is described by the time independent Schrödinger equation. The solutions of the wave-equation are given for regions I-III in Fig. 12b by equations (5), (6), and (7) [Erkoc (2006)]:

$$\psi_I(x) = Ae^{ik_1x} + Be^{-ik_1x} \qquad \frac{\hbar^2 k_1^2}{2m} = E \tag{5}$$

$$\psi_{II}(x) = Ce^{kx} + De^{-kx} \qquad \frac{\hbar^2 k^2}{2m} = V - E > 0 \tag{6}$$

$$\psi_{III}(x) = Fe^{ik_1x} \qquad \frac{\hbar^2 k_1^2}{2m} = E \tag{7}$$

where h is the reduced Planck constant, m is the electron mass, k is the wave number, E is the electron energy, V is the energy required for classical conduction, and A, B, C, D, and F are constants that are defined by the particular system. The wave function describes the probability that an electron will exist at a given location in space. In the classical regions, I and III (outside of the barrier), the electron wave function (ψ_I and ψ_{III}) behavior is sinusoidal, as shown in Fig. 12b. Within the barrier (region II) the amplitude of the wave function (ψ_{II}), decreases exponentially. A transmission coefficient, T, arises from Eqs. (5-7) that is exponentially dependent upon gap distance. Tunneling resistivity (ρ_t) is proportional to the reciprocal of the transmission coefficient, and is given by [Hu, Karube, Yan, Masuda and Fukunaga (2008)]:

$$\rho_t \sim \exp\left(\frac{4\pi d\sqrt{2m\lambda}}{h}\right) \qquad (8)$$

For polymers the barrier height, λ, is approximately 0.5 eV [Hu, Karube, Yan, Masuda and Fukunaga (2008)]. Thus, significant tunneling occurs when the junction gap is less than 1 nm [Kyrylyuk (2008)]. This is illustrated in Fig. 13 with typical values for the parameters of Eq. 8.

The tunneling model may be combined with the single junction FEA calculations to obtain an estimate of resistance as a function of strain for a range of junction parameters. Fig. 14 plots the final resistivity vs. strain and initial gap for two typical nickel strands at 0° misorientation [Johnson, Gardner, Fullwood, Adams and Hansen (2009)]. The results highlight the fact that resistivity across junctions that begin with small separation (near the 1 nm tunneling threshold) decreases only marginally under strain. Junctions that begin with larger separation, on the other hand, exhibit a much greater relative decrease in resistivity. This appears to explain the dramatic piezoresistive behavior of the nano-nickel composite; an immobilized layer of silicone causes junction gaps greater than 1 nm, many of which reduce to below 1 nm under strain, resulting in a sharp reduction in resistivity. In order to consider the macroscopic effects (as opposed to resistivity of single junctions), a percolation model is next employed.

6.5 *Percolation Theory and Scaling Law*

Percolation theory is a common model used to predict conductivity in two phase composites, where one phase is highly conductive, and the other has very low conductivity. Conductivity in a random electrical network follows a power law in the form of [Li, Gao and Fielding (2007), Rakowski and Kot (2005), Sahimi (1983),
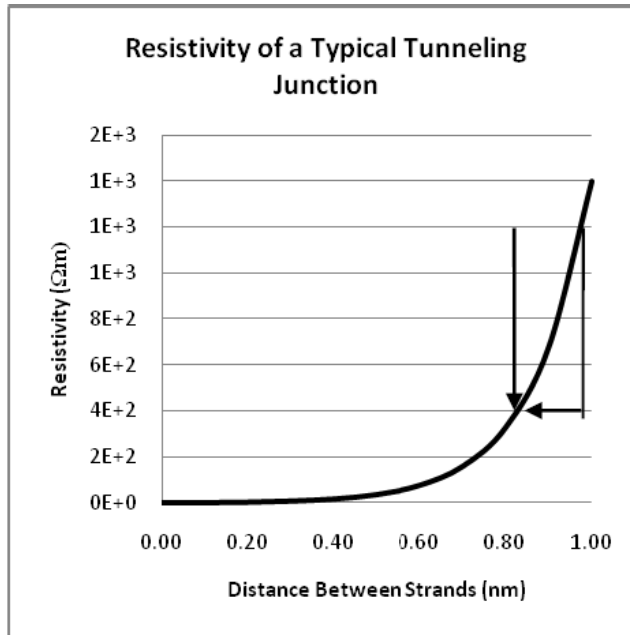
Resistivity of a Typical Tunneling Junction

Figure 13: A small change in distance results in a large change in resistivity.

Taya, Kim and Ono (1998)]:

$$\sigma \sim (p - p_c)^{\tau} \tag{9}$$

(repeated here for clarity) where σ is the macroscopic conductivity, τ is the critical conductivity exponent, p is the volume fraction of the conductive phase, and p_c is the critical volume fraction of the conductive phase at which an infinite percolating cluster is first formed. This model is generally used to predict conductivity with increasing volume fraction of filler material [Domany and Kinzel (1981)]. However, it can also be applied to predict piezoresistivity when used in conjunction with quantum mechanical charge transport phenomena such as tunneling [Sichel, Gittelman and Sheng (1978)]. In this case it is assumed that the volume fraction of nickel is well above the percolation threshold for a nickel composite with conductive junctions. This is known to be the case for 15 vol% nano-nickel from results with other matrix polymers. For this adaptation, the application of strain increases the *number fraction of conductive junctions*, which produces the same result as an increase in *volume fraction of conductive phase*.

As strain is applied to the composite material, the average distance between nickel nanostrands decreases and junctions that were previously too distant for significant
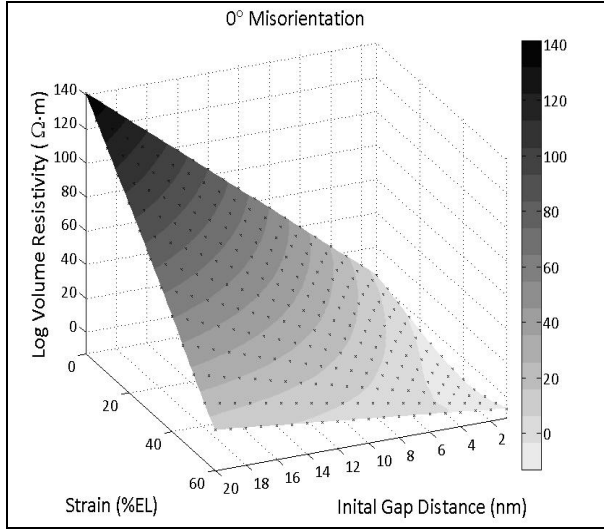
Figure 14: FEA shows that a small change in strain gives a large change in resistivity as predicted by quantum mechanical tunneling. This plot is for two parallel strands.

quantum tunneling come into close enough proximity to begin electrical conduction. If the junction character distribution is known, then the fraction of tunneling junctions that exhibit conductivity above some defined level of strain can be determined using the results of the FEA and analytical models described above. For the sake of this exercise we assume a simple junction character distribution, and suggest future work to improve this model in the conclusions. The model takes a random texture for the junction vector. The junction gap is assumed to be approximated by a Gaussian distribution, $f(d)$, with mean gap above the conduction threshold of 1 nm described above (a specific value of 5 nm is assumed with a standard deviation of 6 nm; again, future work will improve this estimate). As the material is strained the average junction gap decreases and junctions with higher initial gaps become conductive (see Fig. 11). This shifts the distribution towards the origin.

We will define the number of 'conductive' junctions (gaps < 1 nm) as Q. Q is a function of strain (Fig. 15) given by:

$$Q(\varepsilon) = \int_0^{1nm} f(d,\varepsilon) \, dd \qquad (10)$$

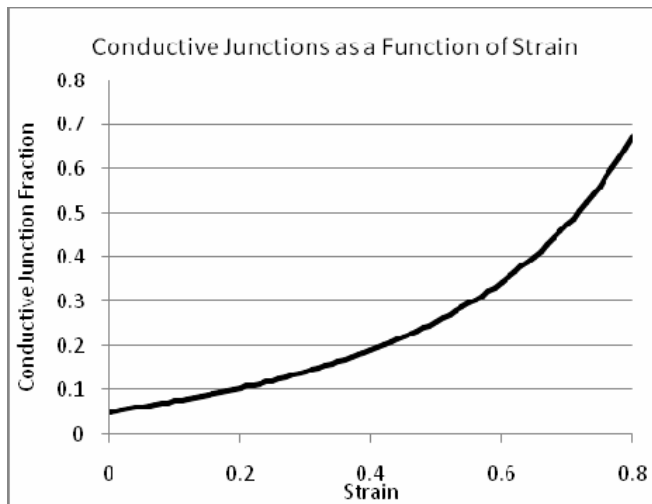Then the composite resistivity is given as a function of strain, and governed by a

Figure 15: Strain creates more conductive junctions in the material.
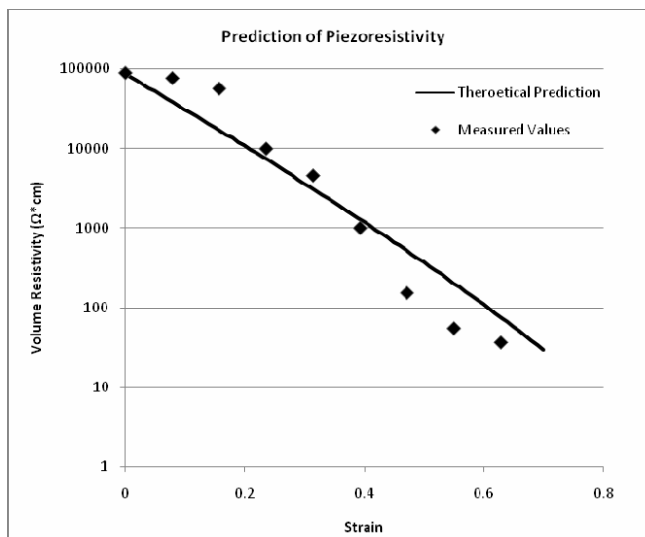

Figure 16: Measured vs. modeled data for piezoresistivty of a 15 vol% nano-nickel composite.

power law:

$$\rho\left(\varepsilon\right) \sim \left(Q\left(\varepsilon\right) - Q_c\right)^{-\tau} \tag{11}$$

Notice that the resistivity of the optimized NiNs-silicone composite at 0 % elongation (on the order of 1×10^3 Ωm) is already orders of magnitude below the resistivity of the silicone itself (on the order of 1×10^{10} Ωm). It is likely that the material is already in the region of the critical fraction (Q_c) of conductive junctions; hence we will assume that only the supercritical percolation behavior need be considered. For our current model, the critical fraction of conductive junctions is assumed to be extremely small. The power law exponent depends only on the dimensionality of the problem and was taken to be $\tau = 2.36$ as suggested by Kirkpatrick [Kirkpatrick (1973)].

In summary, the combined percolation tunneling model proceeds as follows:

1. Assume a random / Gaussian junction character distribution

2. Determine a conduction threshold (taken to be 1 nm from the tunneling model – Fig. 13)

3. Model evolution of junction character using analytical (Eq. 4) and FE analysis

4. Input the fraction of conducting junctions into the percolation model (Eq. 9), solving for the constant of proportionality.

The resulting model does an excellent job of predicting the behavior of the optimized NiNs composite as shown in Fig. 16.

7   Conclusions and Discussion

Nickel nanostrands at an optimized 15 vol% concentration within a silicone matrix demonstrate a dramatic piezoresistive effect with a negative gauge factor. The volume resistivity decreases in excess of three orders of magnitude at a 60% strain level. The piezoresistivity does decrease slightly as a function of cycles but not significantly as a function of time. The material's conductivity is also temperature dependent, once again with a negative dependence.

The evidence indicates that nickel strands are physically separated by matrix even at high volume fractions, and points to a mechanism that involves a large change in conductivity for a small relative position change at nickel junctions. Combined with the temperature dependence data, this suggests a quantum tunneling mechanism with an immobilized layer of matrix material holding nickel strands apart

beyond the highly conductive range for junctions. Based upon a statistical model of junction character distribution, a quantum tunneling-percolation model has been applied that accurately reflects the mechanical and thermal effects.

In order to more accurately determine coefficients for the various equations in the model, future experiments will be performed to quantify the quantum tunneling effect between two nickel electrodes across a silicone barrier. Focused ion beam microscopy has been performed on the nickel nanocomposite as a proof of concept, and this work will be expanded to better quantify the junction character distribution. This data will lead to a refined prediction for the junction character distribution, and resultant piezoresistive effect.

References:

Balberg, I. (2002): A Comprehensive Picture of the Electrical Phenomena in Carbon-Black Polymer Composites, *Carbon*, 40.

Balberg, I. (1987): Tunneling and Nonuniversal Conductivity in Composite Materials, *Phys Rev Lett*, 59, 12, 1305-1308.

Balberg, I., Wagner, N., Goldstein, Y., Weisz, S. Z. (1990): Tunneling and Percolation Behavior in Granular Metals, *Mater Res Soc Proc*, 195.

Bigg, D. M. (1977): Conductive Polymeric Compositions, *Polymer Engineering and Science*, 17, 12.

Bigg, D. M. (1979): Mechanical, Thermal, and Electrical Properties of Metal Fiber-Filled Polymer Composites, *Polymer Engineering and Science*, 19, 16.

Bloor, D., Graham, A., Williams, E. J., Laughlin, P. J., Lussey, D. (2006): Metal-Polymer Composite with Nanostructured Filler Particles and Amplified Physical Properties, *Appl Phys Lett*, 88, 102103.

Choi, K. M., Rogers, J. A. (2003): A Photocurable Poly(dimethylsiloxane) Chemistry Designed for Soft Lithographic Molding and Printing in the Nanometer Regime, *J. Am. Chem. Soc.*, 125, 14, 4060-4061.

Chen, C. J., Hamers, R. J. (1991): Role of atomic force in tunneling -barrier measurements, *J. Vac. Sci. Technol. B*, 9, 2, 503-505.

Dalmas, F., Dendievel, R., Chazeau, L., Cavaille, J. Y., Gauthier, C. (2006): Carbon Nanotube-Filled Polymer Composites. Numerical Simulation of Electrical Conductivity in Three-Dimensional Entangled Fibrous Networks, *Acta Materialia*

Deutsch, M. (1987): An accurate analytic representation for the Bloch-Gruneisen integral, *Journal of Physics A: Mathematical and General*, 20.

Domany, E., Kinzel, W. (1981): Directed Percolation in Two Dimensions: Numerical Analysis and an Exact Solution, *Phys Rev Lett*, 47.

Erkoc, S. (2006): Fundamentals of Quantum Mechanics, *Dallas: Taylor & Francis*.

Gao, X. L., Ma, H. M. (2008): A Three-Dimensional Monte Carlo for Electrically Conductive Polymer Matrix Composites Filled with Curved Fibers, *Polymer*, 49.

Grimmett, G. (1999): *Percolation. 2nd ed.*, Springer, 321.

Grunlan, J. C., Gerberich, W. W., Francis, L. F. (2001): Lowering the Percolation Threshold of Conductive Composites Using Particulate Polymer Microstructure, *J Appl Polym Sci*, 80.

Gul, V. E. (1996): Structure and Properties of Conducting Polymer Composites, *VSP, Utrecht*.

Guo, Z., S Park, H T Hahn, S Wei, M Moldovan, A B Karki, D P Young (2007): Giant magnetoresistance behavior of an iron/carbonized polyurethane nanocomposite, *Appl Phys Lett*, 90, 053111.

Hansen, G. (2007): High Aspect Ratio Sub-Micron and Nano-scale Metal Filaments, *SAMPE Journal*, 41, 2-11.

Hu, N., Karube, Y., Yan, C., Masuda, Z., Fukunaga, H. (2008): Tunneling Effect in a Polymer/Carbon Nanotube Nanocomposite Strain Sensor, *Acta Materialia*, 56.

Jing, X., Zhao, W., Lan, L. (2000): The Effect of Particle Size on Electric Conducting Percolation Threshold in Polymer/Conducting Particle Composites, *J Mater Sci Lett*, 19.

Johnson, O. K., Gardner, C. J., Fullwood, D. T., Adams, B. L., Hansen, G. (2009): *Deciphering the Structure of Nano-Nickel Composites*.

Kirkpatrick, S. (1973): Percolation and Conduction, *Reviews of Modern Physics*, 45, 3.

Kyrylyuk, A. V. (2008): Continuum percolation of carbon nanotubes in polymeric and colloidal media, *Proceedings of the National Academy of Sciences of the United States of America*, 105, 8221-226.

Li, K., Gao, X. L., Fielding, J. C. (2007): *Electrical Conductivity of Nickel Nanostrand-Polymer Composites*, AIAA.

Litvinov, V., Steeman, P. (1999): EPDM-carbon black interactions and the reinforcement mechanisms, as studied by low-resolution H-1 NMR, *Macromolecules*, 32, 25, 8476-90.

Louis, A. A., Sethna, J. P. (1995): Atomic Tunneling from a STM/AFM tip: Dissipative Quantum Effects from Phonons, *Phys. Rev. Lett.*, 74.

McLachlan, D. S., Chiteme, C., Park, C., Wise, K. E., Lowther, S. E., Lillehei,

P. T., Siochi, E. J., Harrison, J. S. (2005): AC and DC Percolative Conductivity of Single Wall Carbon Nanotube Polymer Composites, *Wiley InterScience Online*, 10.1002, 20597.

Mehbod, M., P Wyder, R Deltour, C Pierre, G Geuskens (1987): Temperature Dependence of the Resistivity in Polymer-Conducting-Carbon-Black Composites, *Phys Rev B*, 36, 14.

Nurazreena, Hussain, L. B., Ismail, H., Mariatti, M. (2006): Metal Filled High Density Polyethylene Composites-Electrical and Tensile Properties, *J Thermoplas Comp Mater*, 19.

Radhakrishnan, S. (1994): High Piezoresistivity in Conducting Polymer Composites, *Materials Letters*, 18, 358-62-358-62.

Rakowski, W. A., Kot, M. (2005): Thermal Stress Model for Polymer Sensors, *J Them Stresses*, 28.

Rubin, Z., Sunshine, S. A., Heaney, M. B., Bloom, I., Balberg, I. (1999): Critical Behavior of the Electrical Properties in a Tunneling-Percolation System, *Phys Rev B*, 59, 19.

Sahimi, M. (1983): Critical Exponent of Percolation Conductivity by Finite-Size Scaling, *Journal of Physics C: Solid State Physics*, 16, L521-527.

Schadler, L. S., Giannaris, S. C., Ajayan, P. M. (1998): Load Transfer in Carbon Nanotube Epoxy Composites, *Appl Phys Lett*, 73, 26.

Sichel, E. K., Gittelman, J. I., Sheng, P. (1978): Transport Properties of the Composite Material Carbon-Polyvinylchloride, *Phys Rev B*, 19, 10.

Simmons, J. G. (1963): Generalized Formula for the Electric Tunnel Effect Between Similar Electrodes Seperated by a Thin Insulating Film, *J Appl Phys*, 34, 6.

Stein, J. (1988): Stress relaxation studies of model silicone RTV networks, *J Appl Polymer Sci,* 36,3, 511-521.

Tang, H., Chen, X., Tang, A., Luo, Y. (1996): Studies on the Electrical Conductivity of Carbon Black Filled Polymers, *J Appl Polym Sci*, 59.

Taya, M., Kim, W. J., Ono, K. (1998): Piezoresistivity of a short fiber/elastomer matrix composite, *Mechanics of Materials*, 28, 1-4, 53-59.

Wang, S. F., Ogale, A. A. (1993): Simulation of Percolation Behavior of Anisotropic Short-Fiber Composites with a Continuum Model and Non-Cubic Control Geometry, *Comp Sci and Tech*, 46, 4.

Wescott, J. T., Kung, P., Maiti, A. (2007): Conductivity of Carbon Nanotube Polymer Composites, *Appl Phys Lett*, 90, 033116.

Wymyslowski, A., Santo-Zarnick, M., Friedel, K., Belavic, D. (2004): Numerical Simulation and Experimental Verification of the Piezoresistivity Phenomenon for the Printed Thick-Film Piezoresitors, *5th I.C. on Thermal and Mechanical Simulation and Experiments EuroSImE.*

Zhou, J. F., Song, Y. H., Zheng, Q., Wu, Q., Zhang, M. Q. (2008): Percolation transition and hydrostatic piezoresistance for carbon black filled poly(methylvinylsilioxane) vulcanizates, *Carbon*, 46, 679-691.